Hindawi
Geofluids
Volume 2022, Article ID 3855799, 14 pages
https://doi.org/10.1155/2022/3855799

Research Article

Numerical Modeling of Controlling a Floor Heave of Coal Mine Roadways with a Method of Reinforcing in Wet Soft Rock

Ivan Sakhno, Svitlana Sakhno, Alla Skyrda, and Oksana Popova

Donetsk National Technical University, 2, Shybankova Square, Pokrovsk, Donetsk Region, 85300, Ukraine

Correspondence should be addressed to Ivan Sakhno; ivan.sakhno@donntu.edu.ua

Received 9 October 2022; Revised 17 November 2022; Accepted 21 November 2022; Published 3 December 2022

Academic Editor: Qingquan Liu

A floor heave is usually a serious failure phenomenon in mine roadways, especially in the conditions of a wet soft rock. There are bright prospects for using a method of reinforcing for controlling a floor heave in mine roadways under a dramatic heave. In the current research, a floor heave mechanism in the wet soft rock of mine roadways was investigated while the moisture content of the rocks was increasing. That was done by performing numerical simulations in a finite element analysis software system Ansys and by reinforcing the floor in the shape of inverted arch. It was found that a decrease in the modulus of elasticity of rocks caused by saturation leads to a nonlinear increase in a floor heave. This can be explained by the fact that rocks of the floor become plastic strains. A stable correlation was established between water content and a floor heave of a wet rock. It was found that when the floor is reinforced, the proportion of plastic strains in the soil is significantly reduced. The growth of the modulus of elasticity of rocks in the reinforced zone, caused by reinforcing of the floor in the form of inverted arch, leads to a nonlinear decrease of a floor heave. The effective range of floor reinforcing was established. A reliable relation was established between the ratio of the modulus of elasticity of rocks of the reinforced zone to the modulus of elasticity of the surrounding rock and heaving of reinforced rocks. The obtained results can be used to predict the magnitude of heaving of rocks at their saturation, as well as after they are reinforced.

1. Introduction

The modern tendencies of changing the priorities of the world energy in favor of renewable energy sources have influenced the energy policy in many countries. The course towards decarbonization and "green energy" led to the adjustment of the strategy for the development of the coal industry. However, despite the decline in coal production these days, more than a quarter of the world's energy is provided using coal [1, 2]. The coking coals required by metallurgy are still in high demand on the market. Therefore, improving the efficiency of coal mining is an urgent scientific and applied problem.

The large deformations of the surrounding rock have far-reaching negative effects on stability of the mine roadway and therefore are a serious problem. A particularly unfavorable situation with the stability of roadways is observed at great depths and in soft rocks. For roadway roof and sidewalls, the problem of stability can be solved by additional bolting, shotcreting, and mobile roof supports, whereas a floor heave tends to be a serious failure phenomenon in mine roadways [3, 4].

A floor heave in the mine roadway while extracting coal can exceed 1 meter, especially in conditions of increased water inflows [5–7]. This causes problems with the transport of loads and minerals and the supply of air through the mine roadways and also leads to the risk of injuring miners while they are moving along the mine roadways. Controlling a floor heave is important for the stability of mine roadways and solution to the abovementioned problems [8].

Various hypotheses argue that the floor heave mechanism is a consequence of the following: an increase in volume of rocks during destruction and water saturation, squeezing out of rocks like from under a stamp, transition of rocks into a plastic state, creep, squeezing out of destroyed rocks, and a consequence of the mutual influence of these factors. However, all the hypotheses agree that wetting of the rocks leads to the activation of the floor heave.

Małkowski et al. [9] studied the multiplicity of the factors causing floor heave. To quantify the effect of the different factors on floor upheaval, an analysis of results of in situ measurements carried out in three coal mine roadways at 15 measuring stations was presented. The analyses of the study results show that the floor upheaval always depends on time, on floor rocks' compressive strength, and Young's modulus. In the case of rock mass condition affected by water, it depends on the rock compressive strength reduction after submerging rock in water.

Controlling the floor heave is done by the following:

(i) using the inverted arch support and circular support

(ii) stress relief slot which is cut in the floor of roadway

(iii) technology of reinforcing surrounding rock

In practice, the combinations of the listed methods are often used.

The effectiveness of the inverted arch support and circular support, which is the simplest technical solution, is greatly reduced in wet soft rock conditions. In such conditions, the elements of the roadway support are deformed and squeezed into the roadway. These days, the inverted arch support and circular one are used mainly in main roadways with a minor floor heave [10, 11].

The stress relief slot is cut in the floor of a roadway to reduce stress concentration [12]. The types of slots can be a groove or a hole. In order to make a slot, a blasting method can be used, as well as a drilling and cutting method. A pressure relief groove is cut in the floor in longitudinal axis of the roadway or in two corners on the floor [13]. As a rule, a drilling and blasting method is used for the depressurization hole. The hole is usually located along the longitudinal axis, while its depth is much bigger than that one of the groove and can be several meters deep [13]. This method is technically difficult for implementation; moreover, it is expensive. Therefore, it is not widely used these days.

One of the most perspective methods is the one of reinforcing the floor of a roadway. The reinforced zone in the floor can be in the form of a concrete beam [14] or a vault [3]. A reinforced zone can be formed by pouring resin mixture instead of excavating the floor rock at the excavation stage or injecting it into the rock through boreholes at any stage of the excavation. This method is often combined with reinforcing the floor using rock bolts, both steel and flexible cable ones [15, 16]. Such combined structures are the most effective ones in combating heaving; however, their main disadvantage is their high cost and the need for special equipment.

The prospect of heaving control by rock reinforcing is a very attractive one beyond doubt, but the high efficiency of this method is not always achieved. In wet soft rock conditions, some additional measures and update of reinforcing methods are required. For example, in the works [17, 18], it is shown that the quality of reinforcing increases with dehydration of water-saturated rocks. The studies of the effect of water on the change in heaving were undertaken in the work [19]. Sun et al. and Zhong et al. put forward the technology of reinforcing surrounding rock to realize the floor stability in inclined strata and soft rock [20, 21]. Zhang and Shimada [22] proposed to control floor heave in retained goaf-side gateroad by using grouting reinforcement.

Shimada et al. [17] studied the reinforcement effect of cement grouting materials on the floor by laboratory tests and analytical method. Małkowski et al. [23] on the base of laboratory tests described the changes of geomechanical properties of Carbonifeorus claystones that related to their mineral composition and the time of soaking in water. Geomechanical properties, including the bulk density, Young modulus, Poisson ratio, unconfined compressive strength, durability index, and swelling index, were examined in dry rock samples and in water-soaked samples.

But most studies are based on the results of numerical simulations because there are the best ways to model the magnitudes and spatial distribution of deformations [24]. Zhang et al. and Shimada [22] explored the evolution of stress at the floor of roadways by FLAC3D. Sakhno et al. [7] performed numerical modeling of controlling a floor heave of roadways in wet soft rock by Ansys. Małkowski et al. [24] proposed the new modeling methodology for roadway floor heave on the base of numerical simulation by Phase 2. The modeling covers a dry floor condition in which the parameters of the Hoek-Brown failure criterion are gradually lowered over time, and a waterlogged floor condition, in which the strength and strain parameters of the rocks are gradually reduced in line with their progressive saturation. The consistency between the numerical simulations and the underground measurements reached 90–99%.

The carried out analysis indicates that a dramatic floor heave can occur, as a rule, in wet soft rock conditions. In this case, the most promising way of controlling a floor heave in roadways with a dramatic heave is reinforcing. Improving the quality of floor reinforcing in wet soft rock conditions is a topical scientific task. The best ways to model the floor heave process is numerical simulation.

2. Methods

A mechanistic approach was used in the study. The floor heave mechanism appeared to be a consequence of rock displacements and deformations as a result of changes in the stress-strain state of the rock mass in the vicinity of a mine roadway without physical and chemical transformations in the rock structure. At the same time, a hypothesis was accepted about the formation of a nonelastic zone around the roadway, which was described in detail in the work [25, 26]. The concept of the traditional "three-zone (fracture zone, plastic zone, and elastic zone)" failure model (Figure 1) of the surrounding rock formed by a stress redistribution which was caused by roadway excavation [27] was accepted. During the simulation experiment, the model was simplified to the "two-zone" (plastic failure zone and elastic zone) failure model. From the point of view of the numerical experiment, it is expedient to call the plastic failure zone the pseudoplastic zone, since the simulation of the behavior of rocks in the fracture zone and plastic zone was carried out using the mathematical apparatus of a plastic flow. The correctness and admissibility of such a simplification are

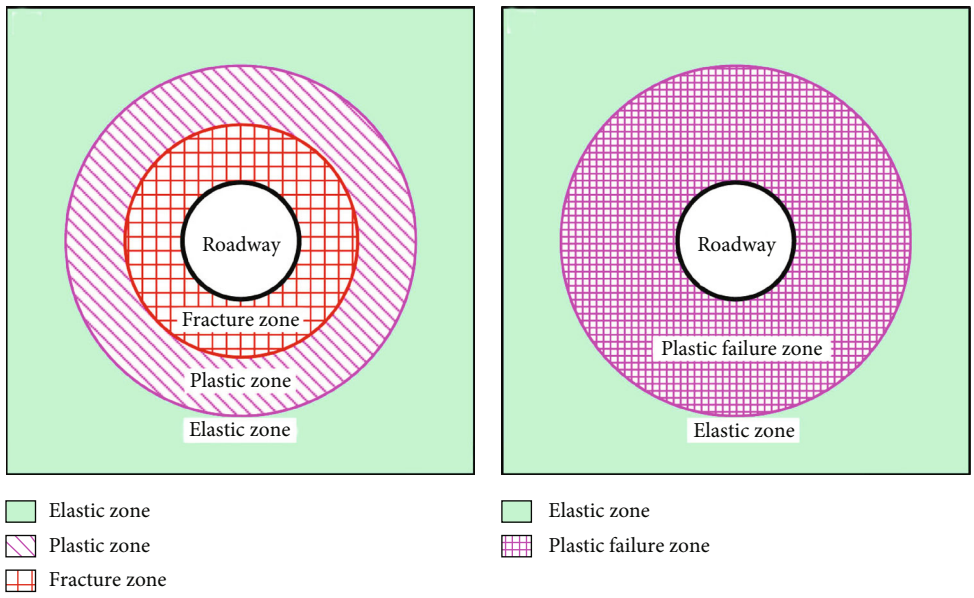

(a) "Three-zone" failure model (b) "Two-zone" failure model

Figure 1: The failure zoning model of the roadway after stress redistribution (from [27] Huang et al., 2020).

substantiated by the general formulation of the problem, the chosen ways for its solution, and the considerations given in the work [27].

The fractional analysis of rocks, carried out by the authors at different coal mines in places of excavation of rock by a dramatic floor heave, enabled us to draw a conclusion that rocks in the fracture zone are mainly represented by a block discrete environment [7]. Under such conditions, a floor heave mechanism is most likely to occur due to the squeezing out of fractured rocks located within the fracture zone into the opening cavity, caused by the growth of a nonelastic zone around the roadway.

The studies were carried out by the authors in the mine Surgaya (Ukraine) at the depth 800 m. They showed that the fracture zone develops alongside with the formation of folds and secondary destruction of rocks, which can be seen in the places where excavation of rock is carried out with a dramatic floor heave (Figure 2).

While conducting a numerical experiment, the abovementioned facts and considerations enable us to conclude that it is correct to take into account the presence of nonelastic zones in the floor by modeling the pseudo plastic zone.

The studies were carried out using numerical modeling in the Ansys finite element analysis software. The simulated rock mass were represented by structurally heterogeneous mudstones. The average uniaxial compressive strength of mudstones was 35-40 MPa. The strata histogram are illustrated in Figure 3.

The surrounding rocks in the pseudoplastic zone were fractured. Therefore, to model rock masses, the mechanical parameters of intact rock were corrected. First of all, this was expressed in a decrease in the modulus of elasticity, the angle of internal friction, and the coefficient of adhesion of the rock masses in the pseudoplastic zone relative to the intact rock. The Hoek-Brown parameters, the geological strength index (GSI), values of the constant mi, and the disturbance factor (D) [28], were used. The geological strength index for surrounding rocks was calculated as GSI = RM R_{89} − 5 [24, 28].

The results of analysis of the floor excavation by dramatic uplift and investigation in the mines geological documentation were used for the determination of the RMR_{89}. Geomechanical parameters of intact rock are as follows: compressive strength of mudstones was 35 MPa, elastic modulus was 4800 MPa, and Poisson's ratio was 0.2. Based on the measurements of joint, the surrounding rocks in situ were determined by Hoek-Brown parameters:GSI = 49, mi = 16, and $D = 0.3$. Geomechanical parameters of rock mass were calculated: compressive strength of mudstones was 1.45 MPa, elastic modulus (E) was 900 MPa, and Poisson's ratio was 0.25.

The modeling was carried out in a volumetric setting on a natural scale. The geometric and physical nonlinearities were taken into account. A standard method was applied to simulate the stress-strain state of the surrounding rocks using the principle of superposition of forces. The analysis of the simulation results was carried out on the basis of processing the stresses, displacements, and strains obtained in the process of numerical modeling. The maximum principal stress theory was adopted as the yield criterion.

The roadway of an arched shape with inclined sidewalls was simulated, around which a nonelastic zone had already been formed. An isolated volume of rock mass was simulated within the pseudoplastic zone. The problem is axisymmetric, so a half of the cross-section of the mine was modeled. A schematic of the model with geometric dimensions is shown in Figure 4(a); the finite element model is shown in Figure 4(b).

The load-bearing capacity of the U-shaped steel support was assumed to be 600 kN. The simulation of the growth in

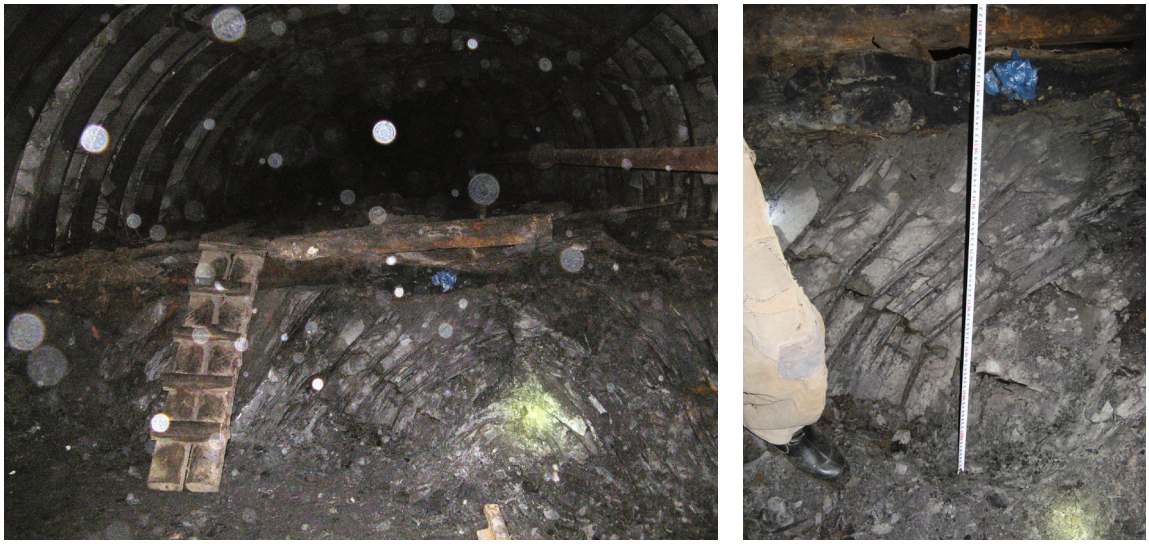

(a) Cross-section of the roadway during the restoration of the cross-section (b) Floor rock structure

Figure 2: Excavation of rock by dramatic floor heave in the mine Surgaya (Ukraine) (authors' photo).

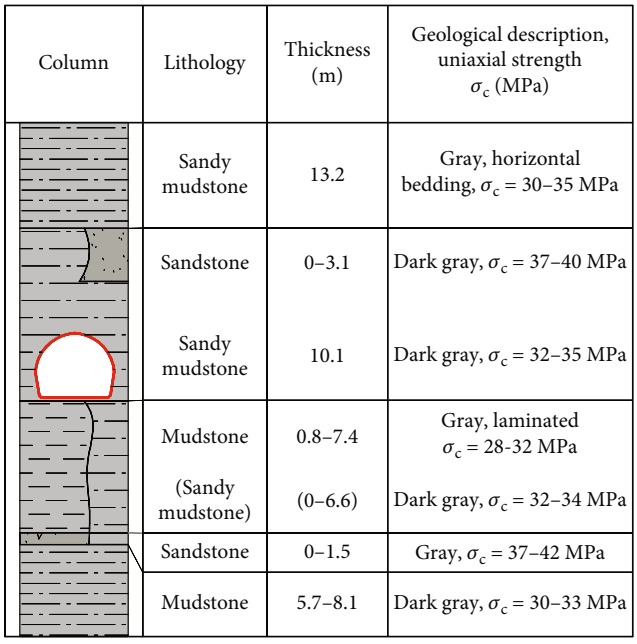

Column	Lithology	Thickness (m)	Geological description, uniaxial strength σ_c (MPa)
	Sandy mudstone	13.2	Gray, horizontal bedding, σ_c = 30–35 MPa
	Sandstone	0–3.1	Dark gray, σ_c = 37–40 MPa
	Sandy mudstone	10.1	Dark gray, σ_c = 32–35 MPa
	Mudstone	0.8–7.4	Gray, laminated σ_c = 28-32 MPa
	(Sandy mudstone)	(0–6.6)	Dark gray, σ_c = 32–34 MPa
	Sandstone	0–1.5	Gray, σ_c = 37–42 MPa
	Mudstone	5.7–8.1	Dark gray, σ_c = 30–33 MPa

Figure 3: The strata histogram.

the size of the pseudoplastic zone due to the transition of rocks to irreversible deformations and dilatancy in the model was carried out by applying external pressure to its contour. It was assumed that the growth of the pseudoplastic zone occurs due to the disturbance of the equilibrium state around the rocks in the process of mining, for example, when a mine gets into the zone of influence of a longwall. The pressure was conventionally assumed to be uniformly distributed and equal to the ultimate strength of the rocks, 35 MPa. The movement of rocks in the direction of the excavation contour resulted in a floor heave. Horizontal displacements at the front and back model boundaries (along the axis of roadway) and at the right boundary were fixed.

In order to simulate the behavior of rocks, the Drucker-Prager deformation model was used. The model enables simulating plastic deformation of rock and its other pressure-dependent material, which corresponds to the properties of rocks in a fracture (pseudoplastic) zone.

The size of the finite element mesh depends on the required accuracy. Near the mine roadway, the size of the finite element is minimal, since high accuracy is important there. On the contour of the model, the stress field is uniform, so the finite elements have the maximum size. This is in line with common practice in numerical simulation in mining. The maximum size of the finite element is 5 m. The minimum size of the finite element is 0.1 m—near the bottom corner of the mine roadway. The minimum size is chosen in an iterative way, thus, to ensure maximum accuracy while avoiding the occurrence of an error in the calculation due to the zero length of the element after deforming.

The model enables simulating plastic deformation of rock and its other pressure-dependent material, which corresponds to the properties of rocks in a fracture zone. The adequacy of the deformation model was established in the course of simulation experiments; the procedure of which is described in detail in the work [29]. The properties of rocks within the pseudoplastic zone are given in Table 1.

In order to assess the effectiveness of reinforcing floor of roadway, a comparison was made between deformations and stresses in models without reinforcing and with reinforcing. The method of reinforcing was fundamentally irrelevant for the solution of the problem. It was assumed that the reinforced zone had the shape of an inverted arch in the roadway floor, and its physical and mechanical properties differed from those of the surrounding rocks.

The geometrical dimensions of the reinforced zone are shown in Figure 3(a), and its physical and mechanical

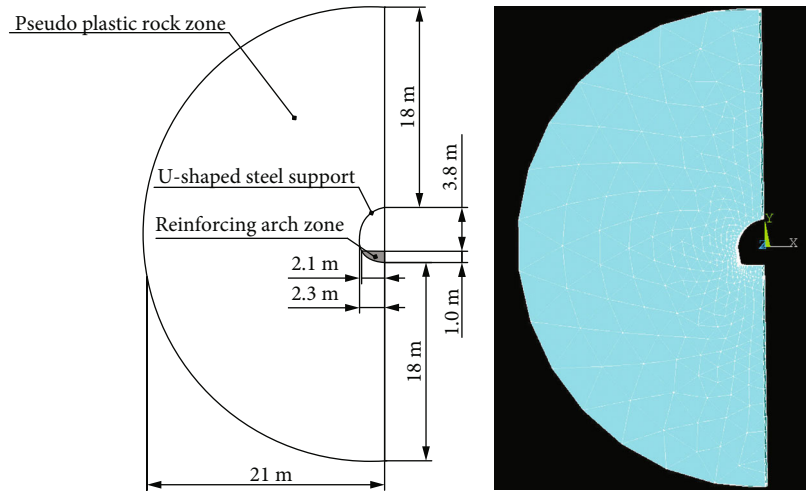

Figure 4: General view of model geometry (a) and finite element model in Ansys (b).

Table 1: Input data for numerical modeling.

No.	Density (kg/m^3)	Elastic modulus (MPa)	Poisson's ratio	Angle of internal friction (deg)	Dilatancy angle (deg)	Cohesion (MPa)
Surrounding rock mass (pseudoplastic zone)						
1	2500	900	0.25	34	34	3
Wet rock mass (pseudoplastic zone)						
2	2500	330-900	0.35-0.25	21-34	21-34	1-3
Reinforced floor rock						
3	2500	1000-9000	0.2	34	34	3-8

properties are shown in Table 1. The value of the elastic modulus in the reinforced zone (E_r) is taken in the range of 1000-9000 MPa (Table 1). It corresponds to the properties of rocks reinforced with resin mixture (while forming a reinforced zone by injection) and the properties of concrete mixtures (while forming a reinforced zone by pouring) [30–33]. Since the physical and mechanical properties of the reinforced zone and the surrounding rocks were different, they were modeled by separate elements of the system.

An increase in humidity in the problem under consideration was taken into account by a decrease in the elastic modulus of wet rock mass (E_{wr}) from 900 MPa to 330 MPa. The range of changes in the modulus of elasticity of rocks, when they are moistened, depends on the well-known results of laboratory experiments to study the effect of water on the physical and mechanical properties of rocks. For example, in works [34–36], a proportional decrease in the modulus of elasticity with moisture saturation of rocks up to 2.2-3.0 times was proved. In addition, the angle of internal friction (from 34 to 21 deg), dilatancy angle (from 34 to 21, deg), and cohesion (from 3 to 1 MPa) were changed, as can be seen from Table 1.

3. Results

The simulation modeling was carried out in three stages:

(1) "Base" model: the analysis of the stress-strain state (SSS) of the rock massive in a dry state without floor reinforcing was done. In this case, the properties of the surrounding rock and reinforced floor were the same, and they were equal to those indicated in Table 1 for the surrounding rock mass

(2) Model "wet rock": the influence of water saturation of rocks on heaving without floor reinforcing was investigated. This was achieved by reducing the modulus of elasticity of the rocks. The surrounding rock and reinforced floor properties were the same, and they were equal to those shown in Table 1 for wet rock mass

(3) Model "reinforced floor": the analysis of the stress-strain state of the massive was carried out during floor reinforcing in the form of inverted arch. A study of the effect of floor reinforcing on heaving was carried out. The properties of the reinforcing floor varied within the range shown in Table 1

During all stages of modeling, the geometry of the model, the dimensions and shape of the finite elements remained unchanged, which made it possible to avoid errors in the interpretation of the results caused by the indicated factors.

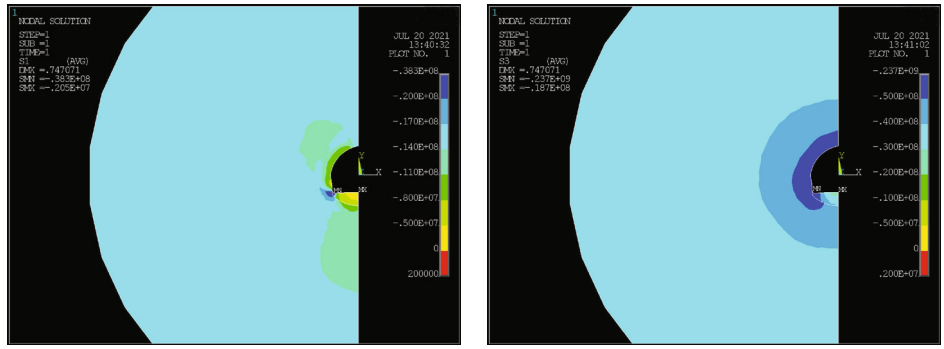

(a) (b)

Figure 5: Maximum (σ_1) (a) and minimum (σ_3) (b) principal stresses around the roadway with the solution "base" model.

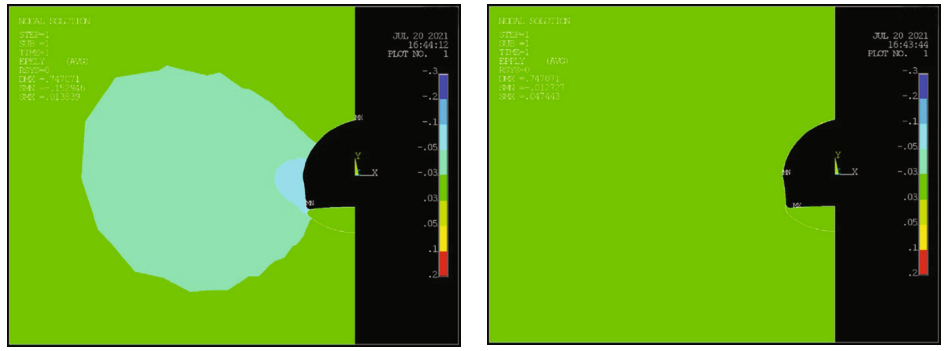

(a) (b)

Figure 6: Vertical elastic (a) and plastic (b) strains around the roadway with the solution "base" model.

The distribution patterns of the max and min principal stresses around the roadway "base" model are shown in Figure 5.

The analysis of the maximum principal stresses σ_1 (Figure 5(a)) enables us to conclude that a zone of reduced stresses is formed in the floor of the roadway at a depth that exceeds half of the roadway width. In the zone, the stress σ_1 is 2-3 times less than outside the area of the roadway influence. Since the rocks within the pseudoplastic zone are not elastically deformed, the presence of a zone of reduced stresses indicates the involvement of the indicated part of the rocks in the process of moving into the roadway cavity. The vertical rise of the floor along the longitudinal axis of the roadway is 0.162 m. The analysis of the distribution patterns of the minimum principal stresses σ_3 (Figure 5(b)) shows that a compression area of more than 50 MPa is formed around the U-shaped steel support, repeating the shape of the support at a distance of up to 1/4 of the roadway width, which can be explained by the resistance of steel support. And also, there is a zone of compression with stresses of 40-50 MPa that is more than the ultimate strength of rocks for uniaxial compression, with a thickness that is equal to 1/2 of the roadway width. In this case, the maxima of the compressive stresses are in the area of the support leg, which is explained by the presence of a natural stress concentrator in the corners on the roadway floor. In the floor of the roadway, a decrease in stresses is observed.

According to the results of testing soft rocks specimen in a volumetric field [34–36] and under uniaxial compression [37–41], it was found that for mudstone, siltstone, argillite, shale, and sandstone with a strength of 25-40 MPa, the failure criteria for strain is about 0.03. The surfaces of elastic and plastic strains are shown in Figure 6. The analysis shows that failure strain in the model is a negative one; they are caused by compression of rocks in the side of the roadway (Figure 6(a)). These strains are elastic. The plastic strains do not reach the failure limit, being in the range of "-0.03"-"+0.03" (Figure 6(b)). Thus, the probability of repeated destruction of rocks in the floor of the roadway is nearly zero.

An increase in humidity significantly changes the picture of the stress-strain state of rocks, which is seen in the "wet rock" solution model. For this model, the patterns of distribution of principal stresses around the roadway at the lowest elastic modulus (330 MPa) from the studied range (Table 1) are shown in Figure 7. In this case, the maximum floor heave of the modeled ones is observed. The vertical rise of the floor along the longitudinal axis of the roadway is 0.663 m. The strain analysis shows that a significant proportion of them are plastic ones (Figure 8).

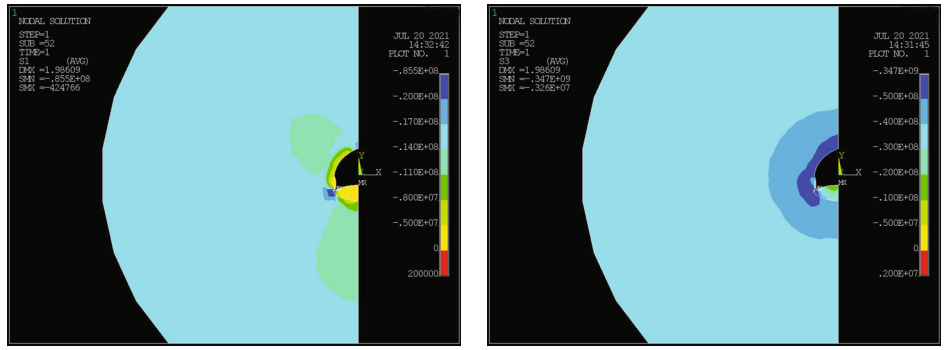

(a) (b)

Figure 7: Maximum (σ_1) (a) and minimum (σ_3) (b) principal stresses around a roadway with a "wet rock" solution model (elastic modulus E_{wr} = 330 MPa).

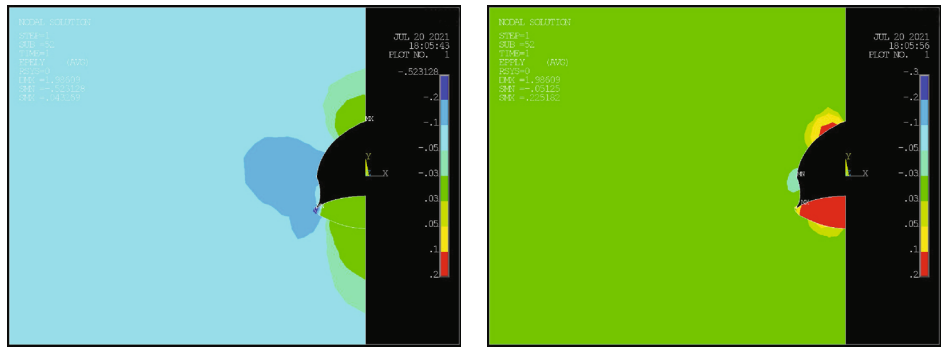

(a) (b)

Figure 8: Vertical elastic (a) and plastic (b) strains around the roadway with a "wet rock" model (elastic modulus 330 MPa).

The evolution of stresses and strains while wetting the rocks can be analyzed by comparing principal stresses (Figures 5 and 7). The analysis of the maximum principal stresses σ_1 shows that the size of the zone of reduced stresses in the floor and the sides of the roadway increases significantly. Such significant deformations occur not only in the floor but also in the sides of the roadway with significant displacement in the area of the support leg. The analysis of the distribution patterns of the minimum principal stresses σ_3 (Figure 8(b)) shows that the compression area of more than 50 MPa around the U-shaped steel support decreased in size to 1/6 of the roadway width, which is explained by the displacement of the roadway contour in the direction of its axis. At the same time, the dimensions of the compression zone with stresses of 40-50 MPa almost did not change. The zone of reduced stress increased both in width and depth.

The analysis shows that failure strains in the model are both positive and negative ones. In the sides of the roadway, they are caused by the compression of rocks and have a minus sign (Figure 8(a)). These strains are elastic ones. In the floor and roof, the failures strain of the roadway are positive. They are mainly plastic strains. They exceed the failure limit by 3-5 times (Figure 8(b)). Thus, the probability of repeated destruction of rocks in the roadway floor is high, which can cause a further increase in heaving of rocks because rocks increase in volume during destruction.

The influence of water saturation of rocks on the amount of heaving can be traced according to the graphs shown in Figures 9 and 10. Along the horizontal axis in Figure 9 shows the half-width of the roadway, where point "0" corresponds to the lower left corner of the roadway and point "2.55" corresponds to the longitudinal axis of the roadway. The control points are shown in Figure 9(a). The nonlinear nature of heaving growth with a decrease in the elastic modulus of the surrounding rocks is clearly seen in the graph (Figure 10) obtained from the results of numerical simulation.

The analysis of graphs (Figure 9) shows that a decrease in the elastic modulus of rocks caused by water saturation results in a nonlinear increase in floor weight. The shape of the roadway contour during the heaving remains unchanged. The maximum floor heave is observed along the roadway axis. The maximum (σ_1) principal stresses in the center of the roadway decrease with decreasing elastic modulus, which is logical. The increase in heaving is a consequence of the transition of rocks to the stage of plastic deformation.

Based on the results of the mathematical modeling, the curve of heaving dependence (H_{fl}) on elastic modulus (E_{wr}) was plotted, which is fairly well approximated by the power dependence $H_{fl} = 1858.3E_{wr}^{-1.368}$ with an approximation reliability $R^2 = 0.99$ (Figure 10). The analysis of the presented graph enables us to conclude that in the studied range, a decrease in the elastic modulus of the surrounding rocks as a

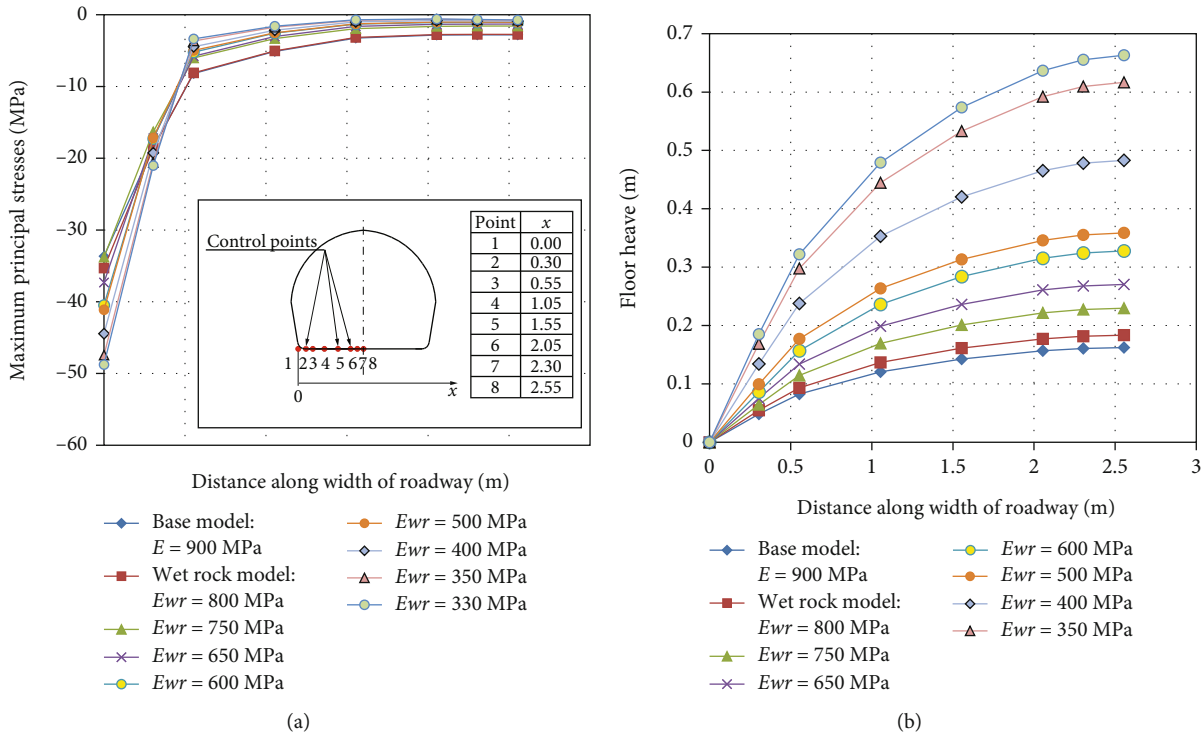

Figure 9: Graphs of the influence of elastic modulus of wet rock (E_{wr}) on the maximum (σ_1) principal stresses (a) and roadway floor heaving (b) according to the results of numerical modeling.

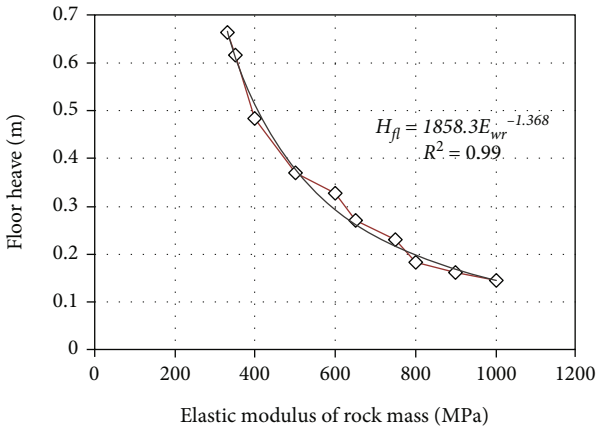

Figure 10: Graph of the dependence of floor heave (H_{fl}) over the axis of the roadway from elastic modulus of wet rock mass (E_{wr}) according to the results of numerical modeling.

result of their threefold water saturation leads to an increase in floor heave by 4.57 times. At the same time, the model does not take into account physical and chemical changes (swelling) in rocks occurring in situ, which will result in an additional increase in heaving.

The reinforcement of the floor rocks leads to a decrease in heaving. Using the solution model "reinforced floor," one can trace how stresses and deformations change around the roadway. Figure 11 shows the distribution patterns of principal stresses around the roadway with an elastic modulus value in the surrounding rocks of 330 MPa. The elastic modulus value in the reinforced zone is assumed to be 4000 MPa. Simultaneously, with the reinforced floor, a sidewall was reinforced in the area of the side arch U-shaped steel support. The vertical rise of the floor along the longitudinal axis of the roadway in this model is 0.339 m, which is 51% less than without floor reinforcement.

The analysis of the maximum principal stresses σ_1 shows that the size and configuration of the low stress zones in the surrounding rocks changed. In the floor of the roadway, the zone of reduced stresses decreased three times compared with the case without reinforcing. Its dimensions tend to be the case presented in the "base model" Figure 5(a). Below the reinforced area in the surrounding rocks, a zone of reduced stress is also formed. At the same time, increased stresses are formed inside the reinforced zone on the side of the surrounding rocks. This area is clearly visible in Figure 11(b), which shows the distribution pattern of the minimum principal stresses σ_3. A compression area of more than 50 MPa is now formed not only around the U-shaped steel support but also on the side of the roadway soil. The dimensions of the compression zone with stresses of 40-50 MPa now repeat the contour of the U-shaped steel support. The effect of reinforcing is clearly seen in the change in the distribution of principal stresses.

The analysis of the distribution of vertical strain shows that the proportion of plastic strain is significantly reduced compared to the situation without reinforcing (Figure 12).

In the sides of the roadway, the failure strains remained practically unchanged, with the exception of the lower

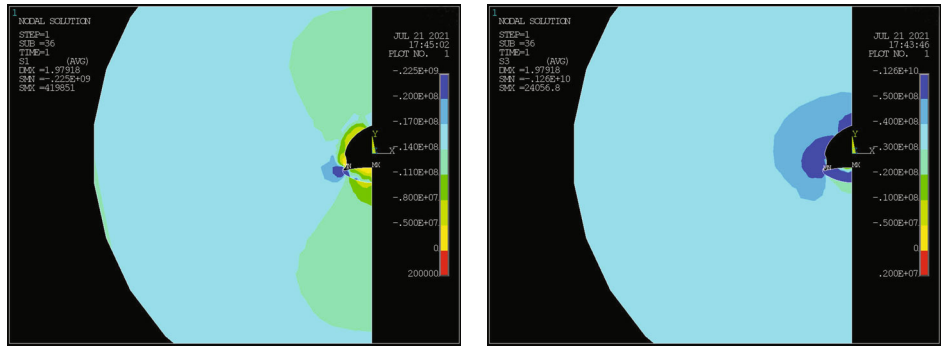

(a) (b)

Figure 11: Maximum (σ_1) (a) and minimum (σ_3) (b) principal stresses around the roadway with a solution model "reinforced floor" (elastic modulus of surrounding rocks E_{wr} = 330 MPa, elastic modulus of reinforcing floor E_r = 4000 MPa).

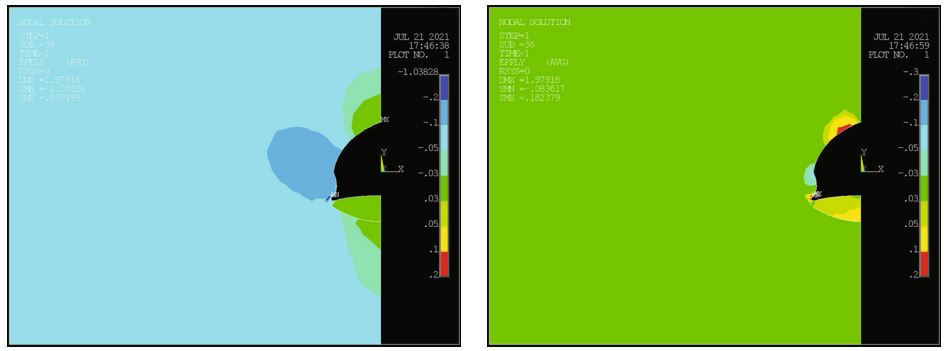

(a) (b)

Figure 12: Vertical elastic (a) and plastic (b) strains around the roadway with a solution model "reinforced floor" (elastic modulus of surrounding rocks E_{wr} = 330 MPa, elastic modulus of reinforcing floor E_r = 4000 MPa).

corner of the roadway. They are predominantly elastic (Figure 12(a)). In the roof of the roadway, the failure strains did not change. They are mostly plastic strains. In the roadway floor, reinforcing led to a significant change in strains. In the boundary part of the reinforced zone with a depth of up to 0.5 m, a slight excess of tensile limit strain is observed, up to 1.5 times. In the lower part of the reinforced zone, at the point of contact with the surrounding rocks, a failure strain is formed, exceeding the tensile limit by up to 3 times (Figure 12(b)). Thus, the probability of destruction of rocks in the near-contour part of the mine is low. The efficiency of reinforcement is obvious.

The effect of reinforcing on the amount of heaving can be traced from the graphs shown in Figure 13.

As an example, the simulation results are presented for the following conditions: elastic modulus of surrounding rocks of 400 MPa and elastic modulus of reinforced floor of 2000-9000 MPa.

Analysis of graphs Figure 13 shows that an increase in the modulus of elasticity of rocks in the reinforced zone caused by reinforcing in the form of an inverted arch leads to a nonlinear decrease in floor weight. The shape of the roadway contour at heaving remains unchanged. The nonlinear nature of the heaving decrease at reinforcing, with different modulus of elasticity of the wet surrounding rock mass, can be seen in the graph Figure 14. The graphs show the effective range of reinforcing.

Figure 14 demonstrates that the high efficiency of reinforcing is observed in the range of elastic modulus of reinforced zone by 3000 MPa. Here, an increase in elastic modulus of reinforced zone by 18% gives a decrease in the roadway floor heave by 58-67%.

4. Discussion

The conducted studies confirm the well-known phenomenon observed onsite, that in the zones of water inflows, the swelling of the floor becomes more active and can exceed 1/3 of the height of the roadway [5–7, 42]. At the same time, the values of the floor heave in such conditions exceed those ones in dry rocks by 3-4 times. Obviously, this is due to a decrease in the deformation modulus of rocks when they are moistened.

To assess the effect of humidity on the floor heave (H_{fl}) value, we introduce a relative indicator—a water increase coefficient (k_w):

$$k_w = \frac{H_{flw}}{H_{fl}}, \quad (1)$$

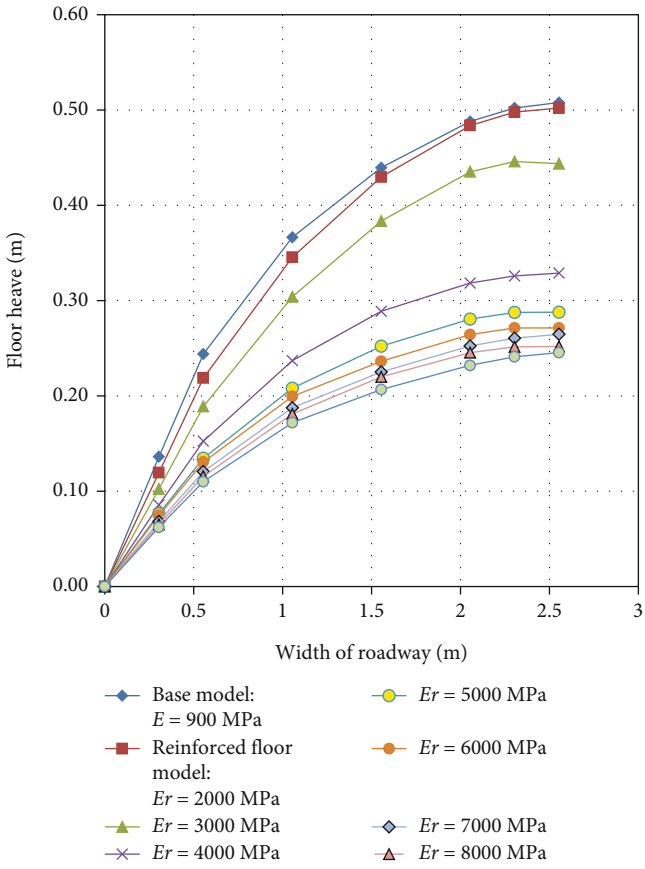

Figure 13: Graphs of the influence of elastic modulus of the reinforced floor rock (E_r) on the roadway floor heave according to the results of numerical modeling.

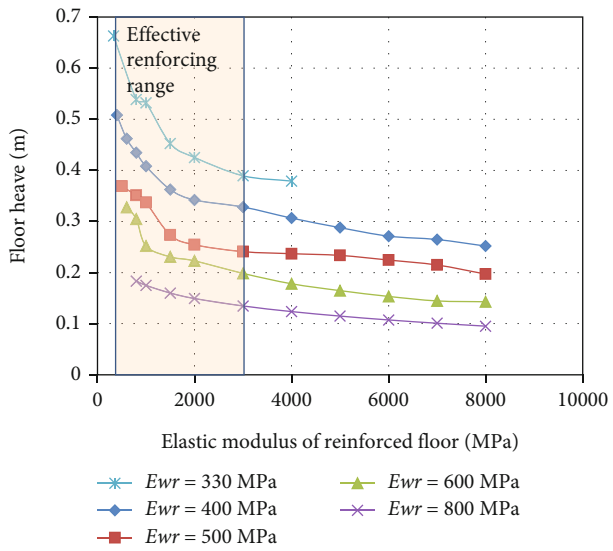

Figure 14: The graph of floor heave value (H_{fl}) along the roadway axis on the elastic modulus of the reinforced zone (E_r) for different variants of elastic modulus of the wet surrounding rock mass (E_{wr}).

where H_{flw} is the floor heave with "wet rock" (m) and H_{fl} is the floor heave with "dry rock" (m).

Variation k_w versus E of the surrounding rocks is shown in Figure 15. When $k_w = 1$, the rocks are dry.

The curve of dependence of water increase coefficient (k_w) on the elastic modulus (E) of rocks is well approximated by the power function $k_w = 11226E^{-1.365}$ with an approximation confidence of $R^2 = 0.986$.

Thus, when one knows the heaving in dry formations, the wet rock heaving (H_{flw}) can be calculated:

$$H_{flw} = k_w \times H_{fl} = 11226E_w^{-1,365} \times H_{fl}\,(\text{m}), \tag{2}$$

where E_w is the elastic modulus with wet rock (MPa).

When one knows the dependence of the decrease in the modulus of elasticity of rocks at water saturation $E_w = f(w)$, it is possible to calculate the floor heave of roadway at different humidity. The dependence for specific surrounding rocks can be established in laboratory experiments. Similar dependences were established many times, for example, in [23, 34–36, 43].

In general, the modulus of elasticity for wet rock (E_w) can be expressed as

$$E_w = k_E \times E\,(\text{GPa}), \tag{3}$$

where k_E is the elastic modulus reduction coefficient and E is the elastic modulus with dry rock (MPa).

As an example to establish the indicated dependence, let us consider some published results of similar experiments. Romana and Vásárhelyi [44] provide an extensive review and discussion of the effect of moisture on compressive strength. Generalizations of the data presented in this article on the dependence of strength on water content, experimental data [45] for shales Linton Lane coal mine and Rye Hill coal mine enabled us to obtain graphs of the dependence of the elastic modulus on water content (Figure 16). In this case, for the transition from strength to elastic modulus, the dependence of uniaxial compressive strength on deformation modulus for rock was used, given in the work [46]:

$$E = 1.6 \times \sigma^{0,75}\,(\text{GPa}), \tag{4}$$

where σ is the rock mass compressive strength (MPa).

Also, Figure 16 shows the results of experiments given in [43]. The analysis of the graphs (Figure 16) shows a clear decrease in the elastic modulus with increasing rock moisture. The effect of water content on elastic modulus is different for different rocks. It is known that the degree of influence of moisture on the mechanical properties of rocks is not the same and primarily depends on the presence of defects and the content of clay particles.

The analysis shows that rocks with a high content of clay particles are most susceptible to water uplift. Such an influence is quite pronounced in mudstones on clay cement.

In order to obtain k_E, we approximate the experimental results for the shale at coal mine Rye Hill [45], shown in Figure 16.

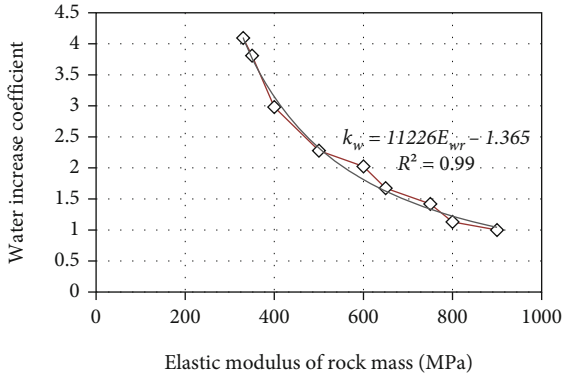

FIGURE 15: The graph of dependence of water increase coefficient (k_w) on elastic modulus (E) of rocks in a wet rock model.

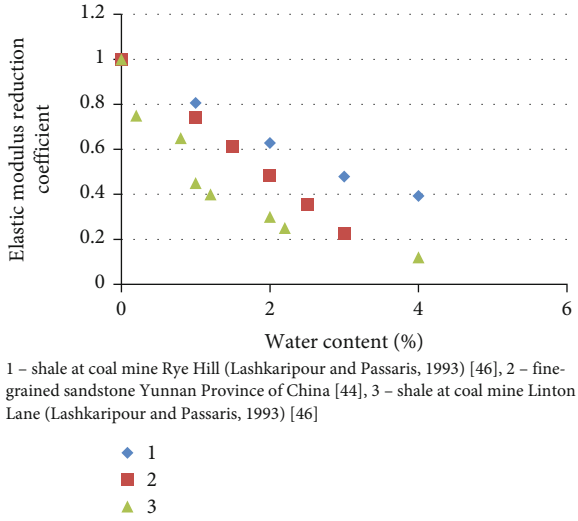

FIGURE 16: Elastic modulus reduction coefficient (k_E) vs. water content (w).

For the coefficient of reliability of approximation $R^2 = 0.997$, the dependence of elastic modulus reduction coefficient (k_E) on water content is described by an exponential function:

$$k_E = 1,0076e^{-0,239\Delta w}, \quad (5)$$

where Δw is the water increase (%).

Thus, wet rock heaving (H_{flw}) for the conditions of shale coal mine Rye Hill [45] can be calculated as

$$H_{\text{flw}} = H_{\text{fl}} \times 11226\left(1,0076e^{-0,239\Delta w} \times E\right)^{-1,365}\,(\text{m}). \quad (6)$$

The obtained dependence can be used to predict the floor heave value with an increase in the moisture content of the rocks. This will enables to timely develop the necessary methods for controlling a floor heave of roadways.

It is a well-known fact that the reinforced floor zone has a positive effect on the stability of the roadways. It is also confirmed by the results of numerical modeling. The decrease of the floor heave at reinforcing is more than 55%. The effectiveness of reinforcing in this case depends on the mechanical properties of the surrounding rocks and the reinforcing zone (Figures 13 and 14).

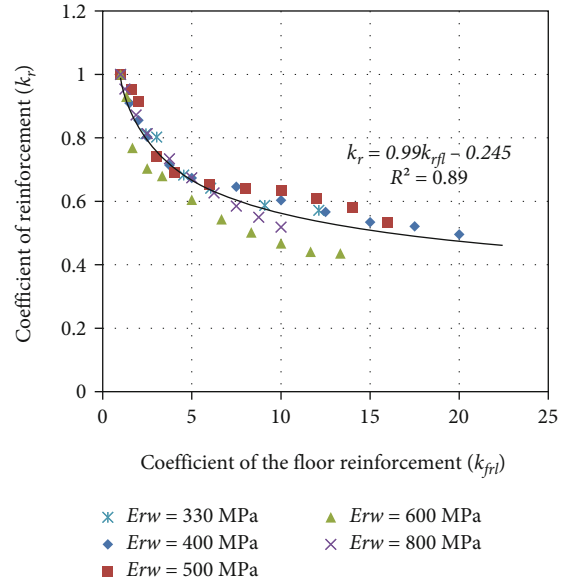

FIGURE 17: Correlations between coefficient of reinforcement (k_r) and coefficient of the floor reinforcement (k_{rfl}) for different elastic modulus of the wet surrounding rock mass (E_{wr}).

As a criterion for the quality of the reinforcing mixture, we take the modulus of elasticity of the reinforced zone. The higher elastic modulus of mixtures tend to be stronger and of better quality. It is known that the higher the reinforcement is, the higher the modulus of elasticity of rocks and reinforcing mixtures is [32, 46]. Let us introduce the relative index of reinforcing—coefficient of the floor reinforcement:

$$k_{\text{rfl}} = \frac{E_{\text{rz}}}{E}, \quad (7)$$

where E_{rz} is the modulus of elasticity of rocks in the reinforced zone (MPa) and E is the modulus of elasticity of the surrounding rocks (MPa).

In order to assess the effect of the modulus of elasticity of rocks in the reinforced zone (E_{rz}) on the amount of heaving of the floor (H_{fl}), let us introduce an indicator—coefficient of reinforcement (k_r):

$$k_r = \frac{H_{\text{flr}}}{H_{\text{fl}}}, \quad (8)$$

where H_{flr} is the heaving after reinforcing (m) and H_{fl} is the heaving without reinforcing (m).

Variation k_r versus k_{rfl} is shown in Figure 17. When $k_r = 1$, there is no reinforcing.

There is a good correlation between the indicators $k_r = 0.9893k_{\text{rfl}}^{-0.245}$ with the coefficient of accuracy of the approximation $R^2 = 0.893$. The analysis of Figure 17 shows that reinforcing of the floor has a similar effect on reducing

displacement at different values of the modulus of elasticity of the surrounding rocks. The effectiveness of reinforcing is very weakly dependent on this indicator. In the investigated range, with a high degree of reliability, it is possible to predict the amount of heaving after the rock reinforcing using the dependence:

$$H_{\mathrm{flr}} = k_r \times H_{\mathrm{fl}} = 0.9893 {k_{\mathrm{rfl}}}^{-0,245} \times H_{\mathrm{fl}}\,(\mathrm{m}). \quad (9)$$

The obtained results can be used to predict the state of development after applying the method of reinforcing for controlling a floor heave of roadways, to select reinforcing mixtures and to substantiate their parameters. At the same time, it is important to underline that the analysis is theoretical and the coefficients in equations (5), (6), and (9) need the calibration in specific mining/geological conditions.

5. Conclusions

In this article, using numerical modeling in the Ansys finite element analysis software, the floor heave mechanism in a roadway under wet soft rock conditions with an increase in rock moisture and reinforcing of the floor in the form of an inverted arch was studied. For this purpose, the distribution patterns of principal stresses and elastic and plastic strains around the roadway were examined. The analysis of the curves of the dependence of the amount of heaving on the moisture content of the rocks, the mechanical properties of the surrounding rocks, and the reinforced zone was carried out. The most important results of this study can be summarized as follows.

According to the studies, it was found that the decrease in the modulus of elasticity of rocks caused by the water saturation leads to a nonlinear increase in floor weight. The nonlinear growth of heaving is a consequence of the transition of rocks to the stage of plastic deformation. In this case, a zone of reduced stresses is formed in the roadway floor and a strain is positive and exceeds the failure limit in tension.

A reliable correlation was established between the water content and the floor heave with wet rock. The obtained dependence can be used to predict the floor heave value with an increase in the moisture content of the rocks. This will enable to timely develop the necessary methods of controlling a floor heave of roadways.

It was found that, as the floor is reinforced, the size and configuration of the zones of reduced stress change. Below the reinforced zone in the surrounding rocks, a zone of reduced stress is also formed. At the same time, increased stresses occur inside the reinforced zone on the side of the surrounding rocks. The proportion of plastic strains is significantly reduced. The growth of the modulus of elasticity of rocks in the reinforced zone, caused by reinforcing the floor in the form of inverted arch, leads to a nonlinear decrease in the floor heave. According to the obtained results, an increase in the deformation modulus of floor rocks as a result of reinforcing leads to a significant decrease of the floor heave. So, for example, reinforcing, which leads to an increase in the modulus of deformation of destroyed floor rocks by 10 times, causes a decrease in heaving by 47-64%. The effective range of the floor reinforcement was established.

In addition to this, a reliable correlation was established between the ratio of the modulus of elasticity of rocks of the reinforced zone to the modulus of elasticity of the rock of the surrounding rock and heaving of the reinforced rocks. This relation with a high correlation coefficient is described by a power function. The obtained results can be used to predict heaving after the implementation of the method of reinforcing to control a floor heave of roadways, the choice of reinforcing mixtures, and the substantiation of their parameters.

Data Availability

The results of numerical simulation data used to support the findings of this study are available from the corresponding author upon request.

Conflicts of Interest

The authors declare that they have no conflicts of interest.

References

[1] H. Ritchie and M. Roser, "Energy," 2020, https://ourworldindata.org/energy.

[2] J. C. Chang and G. X. Xie, "Floor heave mechanism and over-excavation & grouting-backfilling technology in rock roadway of deep mine," *Journal of Mining and Safety Engineering*, vol. 28, no. 3, pp. 361–369, 2011.

[3] J. Wang, Z. Guo, Y. Yan, J. Pang, and S. Zhao, "Floor heave in the west wing track haulage roadway of the Tingnan coal mine: mechanism and control," *International Journal of Mining Science and Technology*, vol. 22, no. 3, pp. 295–299, 2012.

[4] M. Sungsoon, T. Kudret, and S. Serkan, "Management of floor heave at Bulga Underground Operations - a case study," *International Journal of Mining Science and Technology*, vol. 29, no. 1, pp. 73–78, 2019.

[5] Z. Zhu, H. Zhang, J. Nemcik, T. Lan, H. Jun, and Y. Chen, "Overburden movement characteristics of top-coal caving mining in multi-seam areas," *Quarterly Journal of Engineering Geology and Hydrogeology*, vol. 51, no. 2, pp. 276–286, 2018.

[6] P. Gong, Z. Ma, X. Ni, and R. R. Zhang, "Floor heave mechanism of gob-side entry retaining with fully-mechanized backfilling mining," *Energies*, vol. 10, no. 12, p. 2085, 2017.

[7] I. Sakhno, S. Sakhno, and V. Kamenets, "Mechanical model and numerical analysis of a method for local rock reinforcing to control the floor heave of mining-affected roadway in a coal mine," *IOP Conference Series: Earth and Environmental Science*, vol. 970, no. 1, article 012035, 2022.

[8] D. Qian, N. Zhang, D. Pan et al., "Stability of deep underground openings through large fault zones in argillaceous rock," *Sustainability*, vol. 9, no. 11, p. 2153, 2017.

[9] P. Małkowski, Ł. Ostrowski, and Ł. Bednarek, "The effect of selected factors on floor upheaval in roadways-in situ testing," *Energies*, vol. 13, no. 21, p. 5686, 2020.

[10] C. Wang, Y. Wang, and S. Lu, "Deformational behaviour of roadways in soft rocks in underground coal mines and principles for stability control," *International Journal of Rock Mechanics and Mining Sciences*, vol. 37, no. 6, pp. 937–946, 2000.

[11] L. Wu, L. An, and Y. Bai, "In-plane stability of steel circular closed supports with I-section of sinusoidal corrugated webs: experimental and numerical study," *Tunnelling and Underground Space Technology*, vol. 106, no. 8, article 103566, 2020.

[12] Z. Zhang, H. Shimada, T. Sasaoka, and A. Hamanaka, "Stability control of retained goaf-side gateroad under different roof conditions in deep underground y type longwall mining," *Sustainability*, vol. 9, no. 10, p. 1671, 2017.

[13] Z. P. Guo, Z. W. Du, and S. C. Hu, "Comprehensive treatment methods of floor heave disasters in mining areas of China," *Geotechnical and Geological Engineering*, vol. 35, no. 5, pp. 2485–2495, 2017.

[14] X. Lai, H. Xu, P. Shan, Y. Kang, Z. Wang, and X. Wu, "Research on mechanism and control of floor heave of mining-influenced roadway in top coal caving working face," *Energies*, vol. 13, no. 2, p. 381, 2020.

[15] P. Guo and Y. Xin, "Parameters determination and bolting control of gateway floor," *Journal of Coal Science and Engineering*, vol. 17, no. 4, pp. 388–392, 2011.

[16] Q. Chang, H. Zhou, Z. Xie, and S. Shen, "Anchoring mechanism and application of hydraulic expansion bolts used in soft rock roadway floor heave control," *International Journal of Mining Science and Technology*, vol. 23, no. 3, pp. 323–328, 2013.

[17] H. Shimada, A. Hamanaka, T. Sasaoka, and K. Matsui, "Behaviour of grouting material used for floor reinforcement in underground mines," *International Journal of Mining, Reclamation and Environment*, vol. 28, no. 2, pp. 133–148, 2014.

[18] C. Zhu, Y. Wang, M. Chen, Z. Chen, and H. Wang, "Mechanics model and numerical analysis of floor heave in soft rock roadway," *Journal of Coal Science and Engineering*, vol. 17, no. 4, pp. 372–376, 2011.

[19] S. B. Tang and C. A. Tang, "Numerical studies on tunnel floor heave in swelling ground under humid conditions," *International Journal of Rock Mechanics and Mining Sciences*, vol. 55, pp. 139–150, 2012.

[20] X. Sun, F. Chen, M. He, W. L. Gong, H. C. Xu, and H. Lu, "Physical modeling of floor heave for the deep-buried roadway excavated in ten degree inclined strata using infrared thermal imaging technology," *Tunnelling and Underground Space Technology*, vol. 63, pp. 228–243, 2017.

[21] Z. Zhong, Y. Tu, and X. Liu, "Occurrence mechanism and control technology of the floor heave disaster for soft-rock tunnel," *Disaster Advances*, vol. 5, pp. 987–992, 2012.

[22] Z. Y. Zhang and H. Shimada, "Numerical study on the effectiveness of grouting reinforcement on the large heaving floor of the deep retained goaf-side gateroad: a case study in China," *Energies*, vol. 11, no. 4, p. 1001, 2018.

[23] P. Małkowski, Ł. Ostrowski, and P. Bożęcki, "The impact of the mineral composition of carboniferous claystones on the water-induced changes of their geomechanical properties," *Geology, Geophysics & Environment*, vol. 43, no. 1, pp. 43–55, 2016.

[24] P. Małkowski, Ł. Ostrowski, and J. Stasica, "Modeling of floor heave in underground roadways in dry and waterlogged conditions," *Energies*, vol. 15, no. 12, p. 4340, 2022.

[25] M. Abdel-Meguid, R. K. Rowe, and K. Y. Lo, "Three-dimensional analysis of unlined tunnels in rock subjected to high horizontal stress," *Canadian Geotechnical Journal*, vol. 40, no. 6, pp. 1208–1224, 2003.

[26] M. J. Leitman and P. Villaggio, "Plastic zone around circular holes," *Journal of Engineering Mechanics*, vol. 135, no. 12, pp. 1467–1471, 2009.

[27] Y. Huang, A. Zhao, T. Zhang, and W. Guo, "Plastic failure zone characteristics and stability control technology of roadway in the fault area under non-uniformly high geostress: a case study from Yuandian coal mine in Northern Anhui Province, China," *Open Geosciences*, vol. 12, no. 1, pp. 406–424, 2020.

[28] E. Hoek and M. Diederichs, "Empirical estimation of rock mass modulus," *International Journal of Rock Mechanics and Mining Sciences*, vol. 43, no. 2, pp. 203–215, 2006.

[29] I. G. Sakhno, A. V. Molodetskyi, and S. V. Sakhno, "Identification of material parameters for numerical simulation of the behavior of rocks under true triaxial conditions," *Scientific Bulletin of National Mining University*, vol. 5, no. 5, pp. 48–53, 2018.

[30] Y. Sun, G. Li, J. Zhang, and D. Qian, "Experimental and numerical investigation on a novel support system for controlling roadway deformation in underground coal mines," *Energy Science & Engineering*, vol. 8, no. 2, pp. 490–500, 2020.

[31] Y. Sun, J. Zhang, G. Li et al., "Determination of Young's modulus of jet grouted coalcretes using an intelligent model," *Engineering Geology*, vol. 252, pp. 43–53, 2019.

[32] K. G. Kolovos, P. G. Asteris, D. M. Cotsovos, E. Badogiannis, and S. Tsivilis, "Mechanical properties of soilcrete mixtures modified with metakaolin," *Construction and Building Materials*, vol. 47, pp. 1026–1036, 2013.

[33] S. Kosti and D. Vasovi, "Prediction model for compressive strength of basic concrete mixture using artificial neural networks," *Neural Computing and Applications*, vol. 26, no. 5, pp. 1005–1024, 2015.

[34] Z. Qiangui, J. Wenyu, F. Xiangyu, L. Yongchang, and Y. Yang, "A review of the shale wellbore stability mechanism based on mechanical- chemical coupling theories," *Petroleum*, vol. 1, no. 2, pp. 91–96, 2015.

[35] J. F. Yang, L. Li, and H. J. Lian, "Experimental investigation of the effects of water content on the anisotropy of mode I fracture toughness of bedded mudstones," *PLoS One*, vol. 15, no. 8, article e0237909, 2020.

[36] A. D. Alekseev, V. N. Revva, and N. A. Rjazancev, "Razrushenie gornyh porod v obyemnom pole szhimajushhih naprjazhenij," *Naukova Dumka*, vol. 1, p. 168, 1989.

[37] H. Zhou, C. Zhang, Z. Li, D. Hu, and J. Hou, "Analysis of mechanical behavior of soft rocks and stability control in deep tunnels," *Journal of Rock Mechanics and Geotechnical Engineering*, vol. 6, no. 3, pp. 219–226, 2014.

[38] S.-C. Hsu and P. P. Nelson, "Characterization of Eagle Ford Shale," *Engineering Geology*, vol. 67, no. 1-2, pp. 169–183, 2002.

[39] M. Josh, L. Esteban, C. Delle Piane, J. Sarout, D. N. Dewhurst, and M. B. Clennell, "Laboratory characterisation of shale properties," *Journal of Petroleum Science and Engineering*, vol. 88, pp. 107–124, 2012.

[40] O. A. Almisned and N. Alqahtani, "Rock analysis to characterize Saudi soft sandstone rock," *Journal of Petroleum Exploration and Production Technology*, vol. 11, no. 6, pp. 2381–2387, 2021.

[41] Q. Liu, B. Liang, W. Sun, and H. Zhao, "Experimental study on the difference of shale mechanical properties," *Advances in Civil Engineering*, vol. 2021, Article ID 6677992, 14 pages, 2021.

[42] S. Nehrii, S. Sakhno, I. Sakhno, and T. Nehrii, "Analyzing kinetics of deformation of boundary rocks of mine workings," *Mining of Mineral Deposits*, vol. 12, no. 4, pp. 115–120, 2018.

[43] Z. L. Zhou, X. Cai, W. Cao, X. Li, and C. Xiong, "Influence of water content on mechanical properties of rock in both saturation and drying processes," *Rock Mechanics and Rock Engineering*, vol. 49, no. 8, pp. 3009–3025, 2016.

[44] M. Romana and B. A. Vásárhelyi, "Discussion on the decrease of unconfined compressive strength between saturated and dry rock samples," in *Proceedings of the International Society for Rock Mechanics and Rock Engineering 11th ISRM Congress; ISRM:*, pp. 9–13, Lisbon Portugal, 2007.

[45] G. R. Lashkaripour and E. K. S. Passaris, "Correlations between index parameters and mechanical properties of shales," in *8th ISRM Congress, Correlations Between Index Parameters and Mechanical Properties of Shales*, vol. 1, pp. 257–261, Tokyo, Japan, 1993.

[46] J. Li and E. Villaescusa, "Determination of rock mass compressive strength using critical strain theory," in *Proceeding 40th U.S. Symposium on Rock Mechanics*, p. 663, Anchorage, Alaska, 2005.